Correspondence

The Electrocatalysis of O_2 Reduction

AIC70302Z

Sir:

In a recent communication[1] on O_2 electrochemical reduction, Sawyer and Seo state: "On the basis of the body of experimental data in support of mechanistic scheme 1, the one-electron transfer process for reduction of molecular oxygen is concluded to be reversible and independent of electrode materials and solution conditions. The belief that the electrode surface is catalytic for the electron-transfer process is unjustified and not supported by the experimental data." We take exception to these statements and present evidence that the electrochemical reduction of O_2 to $O_2^{-}\cdot$ on some electrode surfaces is catalyzed by the surface.

An illustration of a system involving the electrocatalytic reduction of O_2 to $O_2^{-}\cdot$ and then to HO_2^- is graphite in alkaline solutions. The importance of the surface is demonstrated by the fact that the kinetics of this step are 2 to 3 orders of magnitude slower on the basal plane than on the edge orientation.[2,3] This is not just a matter of true-to-apparent surface areas or semiconductor properties since simple redox couples proceed at reasonable rates on both surfaces. A strong interaction of the O_2 and $O_2^{-}\cdot$ is involved on the edge surface, whereas on the basal plane of graphite such interaction does not occur.

The mechanism proposed for O_2 reduction on the edge orientation of graphite is as follows:[2]

$$O_2 \rightarrow O_2(\text{ads}) \tag{1}$$

$$O_2(\text{ads}) + e^- \rightarrow O_2^{-}\cdot(\text{ads}) \tag{2}$$

$$2O_2^{-}\cdot(\text{ads}) + H_2O \rightarrow O_2 + HO_2^- + OH^- \tag{3}$$

with the first electron-transfer step (eq 2) normally rate controlling. A similar mechanism appears to operate on gold.[4]

Even more striking evidence of an electrocatalytic effect is the large increase in rate constants for O_2 reduction to HO_2^- or H_2O_2 in alkaline and acid solutions observed with monolayer levels of a macrocyclic complex, such as cobalt(II) phthalocyaninetetrasulfonate, adsorbed from the electrolyte onto the basal plane of stress-annealed pyrolytic graphite. Typical results for alkaline solutions, as obtained with the rotating disk electrode, are shown in Figure 1. In this case, the electrocatalysis involves the formation of an O_2 adduct with the strongly adsorbed cobalt macrocyclic complex. If one accepts the concept that O_2 reduction in the solution phase can proceed with O_2 transition-metal complexes as intermediates, then he should also accept the concept of similar surface complexes with such transition-metal complexes bound to an electrode surface.

The data in Figure 1, after correction for diffusion, yield a Tafel plot with a slope of −0.12 V/decade. This is strong evidence that the first one-electron-transfer step is rate controlling, with a symmetrical potential energy barrier corresponding to process 4.

$$O_2 + e^- \rightarrow O_2^{-}\cdot \tag{4}$$

The small currents observed in Figure 1, in the absence of the adsorbed macrocyclic metal complex, are associated with the edge plane exposed at the periphery of the disk plus imperfections or defects in the basal plane surface, separated by distances large compared to the Nernst boundary layer thickness. This accounts for the low values of the diffusion-limiting currents for this surface in Figure 1 and the relatively small sensitivity to rotation rate.

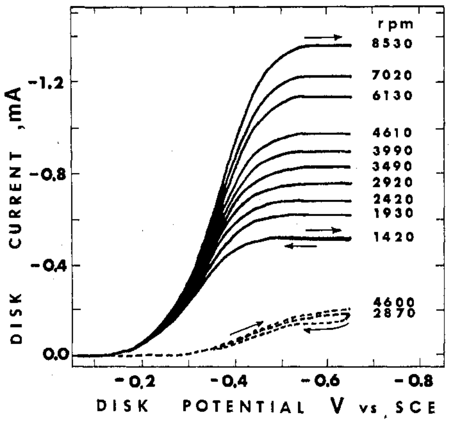

Figure 1. O_2 reduction in 0.1 M NaOH on the rotating disk electrode using the basal plane of stress-annealed pyrolytic graphite with (solid line) and without (dashed line) cobalt(II) phthalocyaninetetrasulfonate adsorbed on the electrode from solution. [Co–TSP solution] 10^{-6} M, electrode area 0.196 cm^2, voltage sweep rate 10 mV s^{-1}, and temperature 20 °C. Rotation rates are indicated on curves in rpm.

Table I. Current Densities with Pure Kinetic Control (i_k) and Apparent First-Order Heterogeneous Rate Constants (k) Determined from Rotating Disk Electrode Data for $O_2 + e^- \rightarrow O_2^{-}\cdot$ at −0.32 V vs. SCE

Electrode surface	Electrolyte	T, °C	i_k, mA cm^{-2}	$k \times 10^3$, cm s^{-1}	Ref
Gold	0.1 M NaOH	26	12	50	4
Graphite edge plane[a]	1 M KOH	22	0.9	4	2
Graphite basal plane (single crystal)	1 M KOH	22	<0.01	<0.04	2
Graphite basal plane[a]	0.1 M NaOH	20	<0.06	<0.24	Present work
Graphite basal plane[a] with adsorbed layer of Co–TSP	0.1 M NaOH	20	3	13	Present work

[a] Stress-annealed pyrolytic graphite.

Sawyer and Seo state that the one-electron transfer process for reduction of O_2 is considered to be reversible and independent of electrode material and solution phase. On the other hand, the kinetic experimental data show instead that this step is rate controlling on various electrode surfaces with the rate constants dependent on the surface material.

Table I compares the current densities and apparent rate constants for O_2 reduction on various surfaces, after correction for mass transport, using the rotating disk electrode technique. For each surface the kinetic studies show the first one-electron-transfer step to be rate controlling. Order-of-magnitude variations in the rate constants are evident in contradiction to the statement of Sawyer and Seo.[1] Whereas Table I lists data for alkaline solutions, large differences also exist in catalytic activity of various electrode surfaces for O_2 reduction in acid and buffered neutral solutions; see, e.g., the work of Kozawa et al.[5] on iron phthalocyanine catalyzed graphite electrodes.

While there is ample evidence that the $O_2 + e^- \rightarrow O_2^{-}\cdot$ process is catalyzed by some electrode surfaces, this is not the main thrust in O_2 electrocatalysis. Rather the search is on for catalysts that promote the direct dissociation of O_2. Some evidence exists that O_2 reduction on Pt, the best catalyst available today, proceeds in this manner.[6-9]

Acknowledgment. The work on O_2 reduction on Pt and macrocyclic transition-metal complexes has been supported by the Electric Power Research Institute and that for O_2 reduction on graphite and Au by the Office of Naval Research. J.Z. holds a fellowship from the Organization of American States.

Registry No. O_2, 7782-44-7; graphite, 7782-42-5; Co–TSP, 28802-06-4.

References and Notes

(1) D. T. Sawyer and E. T. Seo, *Inorg. Chem.*, **16**, 499 (1977).
(2) I. Morcos and E. Yeager, *Electrochim. Acta*, **15**, 953 (1970).
(3) E. Yeager, *Natl. Bur. Stand. (U.S.), Spec. Publ.*, **No. 455**, 203, (1976).
(4) R. W. Zurilla, R. K. Sen, and E. Yeager, submitted to *J. Electrochem. Soc.*
(5) A. Kozawa, V. E. Zillinois, and R. J. Brodd, *J. Electrochem. Soc.*, **117**, 1470 (1970).
(6) M. R. Tarasevich, *Elektrokhimiya*, **9**, 599 (1973).
(7) A. Damjanovic, M. A. Genshaw, and J. O'M. Bockris, *J. Electrochem. Soc.*, **114**, 466, 1107 (1967).
(8) A. Damjanovic, A. Dey and J. O'M. Bockris, *Electrochim. Acta*, **11**, 791 (1966).
(9) J. C. Huang, R. K. Sen, and E. Yeager, "Oxygen Reduction on Pt in 85% H_3PO_4", National Meeting of the Electrochemical Society, Philadephia, Pa., May 8–13, 1977, paper 300; Extended Abstracts, pp 762–763.
(10) On leave from Universidad Tēcnica del Estado, Santiago, Chile.

Chemistry Department
Case Western Reserve University
Cleveland, Ohio 44106

Rajat K. Sen
Josē Zagal[10]
Ernest Yeager*

Received May 2, 1977

Gas-Phase Raman Spectrum of Pentafluorosulfur Chloride, SF_5Cl

AIC70260E

Sir:

The recent paper by Marsden and Bartell[1] has prompted us to report some results that we have obtained concerning the assignments of vibrational frequencies for SF_5Cl.

In earlier work on the vibrational properties of SF_5Cl,[2] Raman bands at 398 and 271 cm^{-1} were assigned to ν_{11}(e) [ρ_w(S–Cl)] and $\nu_6(b_1)$ [$\pi(SF_4)$], respectively. In another study these assignments were reversed.[3] Christe and co-workers[4] commented on the possibility that the band observed at 398 cm^{-1} might be ascribed to the ^{37}Cl component of the S–Cl stretching mode on the basis of force constant calculations and by analogy with SeF_5Cl. Although several workers have accepted this interpretation based on force constant calculations,[1,5] no definitive experimental work has appeared in the literature prior to this report. In a previous paper,[6] we reported the results of a Raman and infrared argon matrix isolation study of SF_5Cl and were able to obtain high-resolution spectra of the bands in the region of 400 cm^{-1} associated with ν_4 (ν(S–Cl)). Since publication of that work, we have obtained polarization data for the Raman spectrum of gaseous SF_5Cl which leave little doubt that the band we observed at 395 cm^{-1} is the ^{37}Cl component of ν(S–Cl).

Spectra were recorded on a Jarrel-Ash Model 500 laser Raman spectrometer equipped with a 5-W Spectra-Physics Model 165 argon ion laser using a multipass gas cell with quartz windows. Other details of the optical system have been described elsewhere.[7] Spectra were observed using 5145- and 4880-Å excitation; the average values of the Raman frequencies are presented in Table I.

Table I. Raman Spectral Data for SF_5Cl(g)

ν, cm^{-1}	I/I_0 [a]	ρ [b]	Assignments[c]	
909.1	3	0.82	ν_8(e)	SF_4 eq square str
951.4	3	0.12	$\nu_1(a_1)$	S–F ax. str
797.2	2	0.44	$2\nu_4(a_1)$	
705.4	93	0.11	$\nu_2(a_1)$	SF_4 eq square str
622.2	6	0.79	$\nu_5(b_1)$	SF_4 eq square str
602.7	3	0.64	$\nu_3(a_1)$	SF_4 out-of-plane def
592.2	2	0.70	ν_9(e)	S–F wag
504.1	2	0.71	$\nu_7(b_2)$	SF_4 in-plane def
440.9	5	0.74	ν_{10}(e)	SF_4 in-plane def
403.8	100	0.16	$\nu_4(a_1)$	S–^{35}Cl str
395.0	47	0.20	$\nu_4(a_1)$	S–^{37}Cl str
273.0	4	0.75	ν_{11}(e)	S–Cl wag

[a] Relative peak heights. [b] Estimated from relative peak heights; curve resolution employed for bands at 403.8 and 395.0 cm^{-1}. [c] Assignments from Cross et al.[2] [except band at 395.0 cm^{-1}].

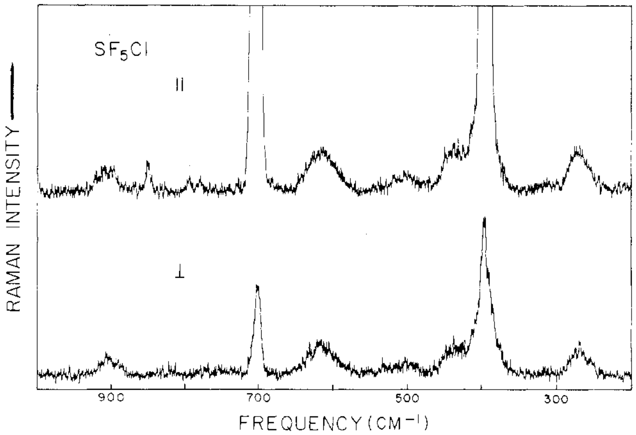

Figure 1. Gas-phase laser-Raman spectrum of SF_5Cl with polarization parallel and perpendicular; 4880-Å excitation (1.3 W), pressure 500 Torr, slits 120 μ, scan speed 0.5 cm^{-1}/s, 1-s time constant, sensitivity 400 Hz.

Raman spectra of SF_5Cl in the gas phase at 500 Torr are shown in Figure 1 under conditions of parallel and perpendicular polarization over the region 200–1000 cm^{-1}. The a_1 modes associated with ν(S–Cl) [ν_4] at 403.8 and 395.0 cm^{-1}, $\nu(SF_4)$ [ν_2] at 705.4 cm^{-1}, and $\nu(S–F_{ax})$ [ν_1] at 851.4 cm^{-1} are still strongly polarized while the band at 602.7 cm^{-1} associated with ν_3 [$\pi(SF_4)$] is weakly polarized. All other bands are depolarized.

A portion of the high-resolution spectrum in the vicinity of 400 cm^{-1} (S–Cl stretch) is shown in Figure 2. The bands shown in Figure 2a are split by approximately 8.8 cm^{-1} and have a relative *integrated* intensity ratio of ca. 3:1. The bands in Figure 2b were observed with the analyzer aligned parallel to the polarization of the incident radiation, and the bands in Figure 2c resulted from scanning the same sample under identical conditions with the analyzer oriented perpendicular to the polarization of the incident radiation. Table I lists the frequencies, relative peak heights, and depolarization ratios for SF_5Cl.

The fact that the Raman band at 395.0 cm^{-1} is strongly polarized indicates that it is due to a mode of symmetry species a_1 and, hence, cannot be assigned to either $\nu_6(b_1)$ or ν_{11}(e). This result and the magnitude of the splitting between the bands at 403.8 and 395.0 cm^{-1} as well as the observed integrated intensities establish the less intense band as the ^{37}Cl component of the S–Cl stretching mode. Moreover, we wish to point out that our observed frequency separation between the S–^{35}Cl and S–^{37}Cl stretching vibrations of 8.8 cm^{-1} in the gas phase (8.2 cm^{-1} in the argon matrix) agrees very well with